

# REMOTE SENSING REQUIREMENTS DEVELOPMENT: A SIMULATION-BASED APPROACH

V. Zanoni<sup>a</sup>, B. Davis<sup>a</sup>, R. Ryan<sup>b</sup>, G. Gasser<sup>c</sup>, S. Blonski<sup>b</sup>

<sup>a</sup> Earth Science Applications Directorate, National Aeronautics and Space Administration, Bldg. 1100, John C. Stennis Space Center, MS 39529 USA – (bruce.davis, vicki.zanoni)@ssc.nasa.gov

<sup>b</sup> Remote Sensing Directorate, Lockheed Martin Space Operations – Stennis Programs, Bldg. 1105, John C. Stennis Space Center, MS 39529 USA – (robert.ryan, slawomir.blonski)@ssc.nasa.gov

<sup>c</sup> Information Systems Directorate, Lockheed Martin Space Operations – Stennis Programs, Bldg. 1110, John C. Stennis Space Center, MS 39529 USA – gerald.gasser@ssc.nasa.gov

## Commission I, WG I/2

**KEY WORDS:** Simulation, Hyper spectral, Multispectral, Resolution, Radiometric, Registration, Spectral, Requirements

### ABSTRACT:

Earth science research and application requirements for multispectral data have often been driven by currently available remote sensing technology. Few parametric studies exist that specify data required for certain applications. Consequently, data requirements are often defined based on the best data available or on what has worked successfully in the past. Since properties such as spatial resolution, swath width, spectral bands, signal-to-noise ratio (SNR), data quantization and band-to-band registration drive sensor platform and spacecraft system architecture and cost, analysis of these criteria is important to optimize system design objectively. Remote sensing data requirements are also linked to calibration and characterization methods. Parameters such as spatial resolution, radiometric accuracy and geospatial accuracy affect the complexity and cost of calibration methods. However, few studies have quantified the true accuracies required for specific problems. As calibration methods and standards are proposed, it is important that they be tied to well-known data requirements. The Application Research Toolbox (ART) developed at the John C. Stennis Space Center provides a simulation-based method for multispectral data requirements development. The ART produces simulated datasets from hyperspectral data through band synthesis. Parameters such as spectral band shape and width, SNR, data quantization, spatial resolution and band-to-band registration can be varied to create many different simulated data products. Simulated data utility can then be assessed for different applications so that requirements can be better understood.

## 1. INTRODUCTION

The accuracies and specifications of remote sensing data will determine the design and cost of a remote sensing system. Parameters such as signal-to-noise ratio (SNR), ground sample distance (GSD) and data quantization will impact sensor design, data storage, communications, and processing architectures and costs. Remote sensing calibration and characterization methods and instruments are also driven by the accuracy of the data being studied. For example, an absolute radiometric accuracy requirement of 3 percent in an image dataset will drive the need for the same level of calibration accuracy for both laboratory and vicarious calibrations. This will in turn affect the cost and complexity of calibration and characterization approaches and procedures. A thorough understanding of required calibration accuracies is therefore required before developing and performing calibration procedures. Parametric studies through data simulation can help to optimize data requirements prior to instrument design or data acquisition. In addition, physics-based simulation can offer an additional role in the cross-comparison verification and validation of remote sensing systems.

The NASA Stennis Space Center (SSC) in Mississippi has developed the Applications Research Toolbox (ART), a group of data simulation algorithms designed to support systematic studies of remote sensing data requirements. The ART software provides the capability to generate simulated multispectral images with predefined properties from existing data with higher spatial and spectral resolution. Multiple

datasets simulated with key data characteristics varied parametrically can be then evaluated by potential end-users for utility in real-world applications.

## 2. FUNCTIONAL OVERVIEW

The ART data simulation process begins by identifying an input dataset. Typically, the input data is very high spatial resolution hyperspectral or multispectral imagery. The first step in the data simulation process is spectral band synthesis, which is the process of combining several hyperspectral bands to create one multispectral band. In the next step, band-to-band misregistration artifacts may be added to simulate sensor artifacts introduced during data acquisition. Next, the spatial degradation or spatial synthesis algorithm is applied to convert the input image GSD and/or point spread function (PSF) to the GSD and PSF of the targeted sensor. Noise may then be added to the simulated image by applying a two-point noise equivalent radiance random noise algorithm. Because of the heavy numerical processing, the data precision of the resultant image is usually not at the simulated sensor's desired level. Therefore, an algorithm is applied to convert the quantization of the processed image (normally 32-bit floating point) to the target sensor's quantization level. Depending on the intent of the simulation study and on the type of input data, some or all of these steps may be performed. The next section describes each step in detail (Gasser, 2001).

### 3. ALGORITHMS

#### 3.1 Spectral Band Synthesis

The simulation of a wide-band multispectral sensor using a narrow-band hyperspectral sensor is achieved by using a linear combination of the hyperspectral sensor responses, normally Gaussian in nature, to create a wide-band spectral response (represented by a spectral response curve). In this process, each band of a multispectral image is simulated by a weighted sum of the hyperspectral image bands. Differences between the ART spectral synthesis algorithm and other methods are in the ways the weights are determined (Blonski et al., 2002). In the ART approach, calculation of the weights is based on finding the best approximation of a multispectral response by a linear combination of the hyperspectral responses. This method is consistent with the goal of accurately modeling a sensor with a predefined spectral response.

To illustrate, consider a multispectral instrument (MSI) with  $N_{MSI}$  bands and a hyperspectral instrument (HSI) with  $N_{HSI}$  bands. The spectral response of the  $i^{\text{th}}$  MSI band  $R_i^{MSI}$  is defined at  $n$  wavelengths  $\lambda_k$ . Spectral response of the  $j^{\text{th}}$  HSI band  $R_j^{HSI}$  is also known for these wavelengths. The linear combination coefficients  $c_{ij}$  are derived by solving the following set of band-synthesis equations in the least-squares sense:

$$R_i^{MSI}(\lambda_k) = \sum_{j=1}^{N_{HSI}} c_{ij} R_j^{HSI}(\lambda_k) \quad \text{for } k=1, \dots, n; \quad i=1, \dots, N_{MSI} \quad (1)$$

Spectral responses of existing hyperspectral instruments, such as the Airborne Visible/Infrared Imaging Spectrometer (AVIRIS) and Hyperion, are accurately approximated with Gaussian functions. For the HSI bands with the Gaussian shape and full width at half-maximum  $\Delta_j$ , the coefficients  $c_{ij}$  are used in the following weighted-sum formulae to calculate (for each pixel) spectral radiance of the synthesized multispectral image bands  $L_i^{MSI}$  from the hyperspectral radiances  $L_j^{HSI}$ :

$$L_i^{MSI} = \frac{\sum_{j=1}^{N_{HSI}} c_{ij} \Delta_j L_j^{HSI}}{\sum_{j=1}^{N_{HSI}} c_{ij} \Delta_j} \quad \text{for } i=1, \dots, N_{MSI} \quad (2)$$

An example of the band synthesis is shown in Figure 1 for the case of Landsat 7 Enhanced Thematic Mapper Plus (ETM+) Band 1 simulated from AVIRIS 1999 data. The figure also illustrates that although the synthesized bands and the actual bands closely overlap, some artifacts do occur, such as ripples at band plateaus, shoulders at band edges and negative values outside bands. Applying the ART spectral band synthesis approach to an AVIRIS image produces a simulated image whose radiance values are consistent with the radiance values of a coincident Landsat 7 image when atmospheric radiative transfer effects are taken into account (Blonski et al., 2002).

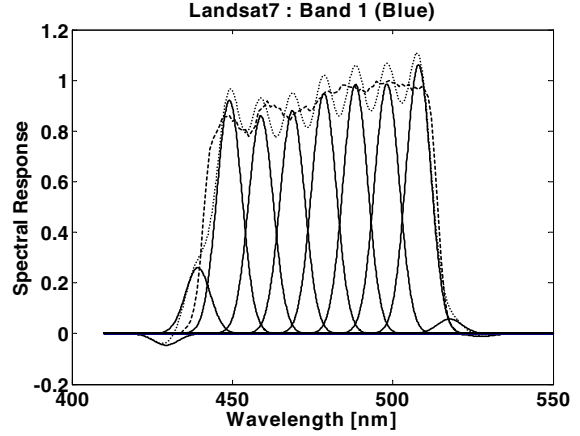


Figure 1. Comparison of actual (dashed) and simulated (dotted) spectral response of Landsat 7 ETM+ band 1; hyperspectral AVIRIS components used in the band synthesis are shown as solid lines.

#### 3.2 Band-to-Band Misregistration

The ART provides a mechanism for introducing the effects of band-to-band misregistration into simulated image products. The misregistration method allows users to shift pixels of the band of interest in the column (left/right) and/or row (up/down) directions. A new image is created that is clipped by the number of rows and/or columns shifted. For the band of interest, clipping takes place on the image edges in the direction of shift, and all other bands are clipped on the edges opposite to the direction of shift. When more than one band is shifted, the output image is the union of all clipped bands. It is recommended that spatial synthesis/degradation (described in the following section) be performed after the band-to-band misregistration procedure. Figure 2 illustrates a simple example where only one band is shifted. The resultant image will always be smaller than the original image. This fact must be taken into account when comparing the misregistered image to the original image (Gasser, 2001).

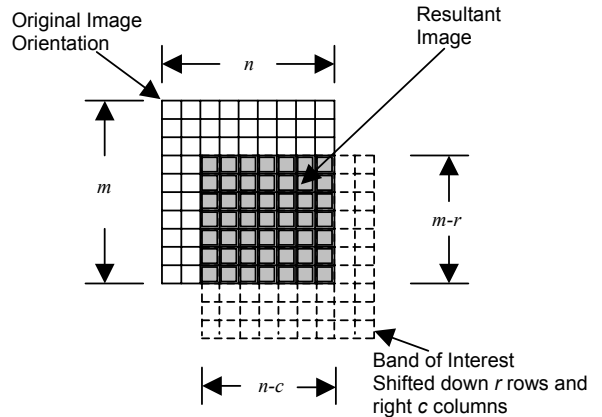


Figure 2. Band-to-band misregistration for a single band.

### 3.3 Spatial Resolution Simulation

Spatial resolution simulation processing converts the input image's GSD to the desired sensor's GSD. Ground sampling distance refers to the size of an image pixel and is a function of the instantaneous field of view (IFOV) and altitude of the sensor. It should be noted that in-track and cross-track pixel size is not necessarily the same, particularly for sensors with a wide field of view. The ART provides two methods of spatial simulation: spatial point spread function synthesis and spatial degradation (Gasser, 2001).

**3.3.1 Point Spread Function Synthesis:** The simulation of a sensor with a low-resolution GSD using a high-resolution GSD sensor is achieved by using a linear combination of the high-resolution sensor's point spread functions (normally Gaussian in nature) to create a low-resolution point spread function. The algorithm is similar to the spectral synthesis algorithm discussed in section 3.1, but it is extended to two dimensions. The coefficients are now  $c_{ijkl}$ , where the  $i$  and  $j$  subscripts are the number of rows and columns of the high-spatial-resolution image and the subscripts  $k$  and  $l$  are the number of rows and columns of the low-spatial-resolution image. Consider the low-resolution sensor Landsat 7 and the high-resolution sensor AVIRIS. Assuming the PSFs are separable in the  $X$  and  $Y$  directions, the following equations can be used to express an effective PSF of the Landsat image as a linear combination of the AVIRIS image PSF:

$$PSF'(x - x_i, 0) = \sum_j b_{jl} PSF_X(x - x_j) \quad (3)$$

$$PSF'(0, y - y_k) = \sum_i a_{ik} PSF_Y(y - y_i) \quad (4)$$

$$c_{ijkl} = a_{ik} b_{jl} \quad (5)$$

These coefficients  $c_{ijkl}$  are found independently for each Landsat pixel by solving, in the least squares sense, the equations (3) and (4) for a given set of points  $(x, y)$ . In current ART simulations, the PSFs are modeled with two-dimensional Gaussian functions. The range of summations in the equations is limited to the region in which each of the PSF components exceeds a threshold value. In the ART, the threshold is currently set to 0.01 (1 percent). Application of this algorithm for one of the pixels in the low-spatial-resolution Landsat image generates plots of the horizontal and vertical point spread functions shown in Figure 3.

For each spectral band, the Landsat image ( $L'$ ) is simulated by linear combination of the AVIRIS image ( $L$ ) pixels according to equation (6).

$$L'_{kl} = \frac{\sum_i \sum_j c_{ijkl} L_{ij}}{\sum_i \sum_j c_{ijkl}} \quad (6)$$

This PSF simulation process is a computationally intensive operation, even for moderately sized images. Using reasonably

equipped computer hardware, processing has taken up to several hours per band for typical images (Gasser, 2001).

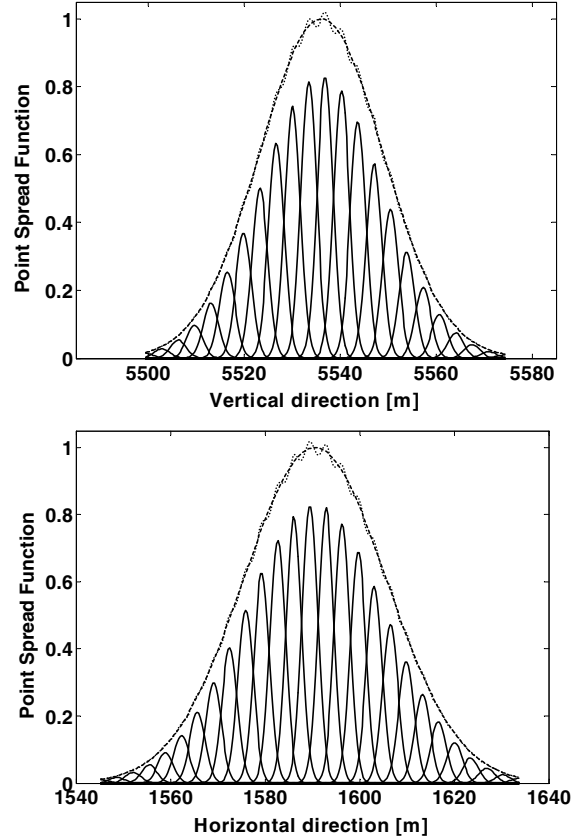


Figure 3. ART PSF synthesis example showing Landsat 7 PSF (dashed), AVIRIS PSF components (solid), and simulated Landsat (dotted).

**3.3.2 Spatial Degradation:** As an alternative to the highly computational process described above, it is useful to have a high-speed spatial simulation algorithm that can produce results in a timely fashion. The ART spatial degradation algorithm uses a combination of low pass filtering (LPF) and resampling techniques to simulate spatially the desired image product. Low pass filtering is achieved by convolving an image with an averaging kernel of  $M \times N$  dimensions (usually square). This allows the user to create an image with the blur characteristics of the desired sensor (Gasser, 2001).

Resampling is performed by choosing a single pixel from an  $N \times N$  block of pixels within the image to represent that entire block of pixels (Gasser, 2001).

### 3.4 Noise

The ART noise algorithm is based on the two-point noise equivalent radiance (NER) model shown in equation (7). To calculate NER for an arbitrary input radiance ( $L_0$ ), NER values ( $NER_L$  and  $NER_H$ ) must be supplied for each band of the sensor at two radiance levels: low ( $L_L$ ) and high ( $L_H$ ).

$$\begin{aligned}
 \text{NER}(L_0) &= \\
 &= \sqrt{\frac{\text{NER}_L^2 L_H - \text{NER}_H^2 L_L - (\text{NER}_L^2 - \text{NER}_H^2) L_0}{L_H - L_L}} \quad (7)
 \end{aligned}$$

Noise is simulated by adding to each band of the radiance image a matrix of random numbers with normal distribution, zero mean, and standard deviation equal to the NER calculated specifically for each pixel (Gasser, 2001).

$$L = L_0 + \text{NER}(L_0) \cdot \text{rnd}(\mu = 0, \sigma = 1) \quad (8)$$

### 3.5 Data Quantization

Data quantization refers to the process by which data with one precision is converted to data with another precision, usually lower than the initial precision. This allows the user to convert the simulated data set to the data quantization level and data storage type of the desired sensor. For example, image pixels with an effective precision of 24 bits and stored as 32 bit floating point numbers can be converted to image pixels with a precision of 12 bits and stored as 16 bit integers. Note that the  $N$ -bit image can be stored in more than  $N$  bits (for example, a 12-bit image stored as 16-bit integers). In such a case, the maximum image value is not the largest integer value of the storage unit, it is based on the value of the maximum digital number,  $DN_{\max}$  (or maximum radiance,  $L_{\max}$ , for radiance images). Data quantization in the ART is accomplished using the equation listed below.

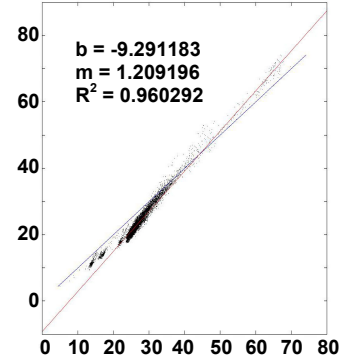
$$DN = \left[ DN_{\min} + (L - L_{\min}) \frac{DN_{\max} - DN_{\min}}{L_{\max} - L_{\min}} \right]_{\text{INT}} \quad (9)$$

$DN_{\min}$ ,  $DN_{\max}$ ,  $L_{\min}$ , and  $L_{\max}$  represent the minimum digital number, maximum digital number, minimum radiance, and maximum radiance values, respectively, and INT indicates the truncation to an integer function (Gasser, 2001).

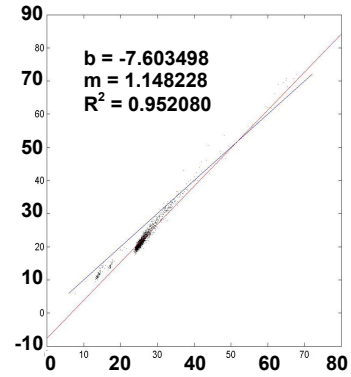
## 4. EXAMPLES

### 4.1 ART Validation Using Landsat

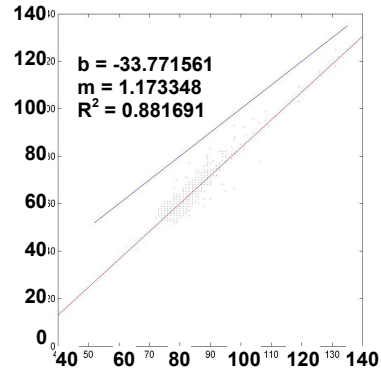
The ART algorithms and selected simulated products have been validated using actual Landsat 7 ETM+ scenes acquired nearly coincident to the input dataset. In one example, an AVIRIS scene of the Department of Energy Savannah River Site in South Carolina acquired on July 26, 1999, was used as an ART input dataset for simulation of several Landsat-like products. The AVIRIS data, acquired at approximately 3-meter GSD, had ART spectral, spatial and noise algorithms applied. Several variations of spatial degradation were explored using different combinations of low pass filtering and resampling. Simulated products were then compared to Landsat 7 ETM+ data acquired near coincidentally. The resulting radiance scatter-plots for two of the products and for ETM+ are shown in Figure 4.



(a) 30-meter LPF applied at 10-meter intervals (10-meter GSD)



(b) 30-meter LPF applied at 30-meter intervals (30-meter GSD)



(c) Landsat ETM+

Figure 4. Comparison of radiance scatter plots for ART simulated data (a and b) and for Landsat 7 data (c), Landsat band 1 vs. band 2.

### 4.2 Sensor Cross-Comparisons

ART simulations have been used to perform sensor cross-comparisons for performance characterization. IKONOS images were used to simulate four VNIR bands of Landsat 7 ETM+ images. Both IKONOS and Landsat 7 images were of similar processing level (radiometric correction, georeferenced with cubic-convolution resampling, UTM projection) and were acquired on June 30, 2000. For each spectral band, the Landsat 7 image was simulated by a linear combination of the IKONOS image pixels, as described in section 3.3.1, to create a simulated Landsat product. Simulated products were compared

with the coincident Landsat 7 images to provide insights on radiometric calibration, spatial resolution and geolocation accuracy of the IKONOS image products. Slight differences between IKONOS and Landsat 7 spectral bands were not addressed.

To perform radiometric comparisons, IKONOS initial post-launch radiometric calibration coefficients were applied to the IKONOS image prior to spatial synthesis. The resulting simulated image radiance values were compared to the well-calibrated Landsat 7 radiance values. The results revealed an inconsistency between IKONOS and Landsat 7 radiometry as shown for the NIR band in Figure 5. This simulation validated similar results derived from vicarious calibration methods. The IKONOS radiometric calibration coefficients were subsequently updated (Blonski, 2001).

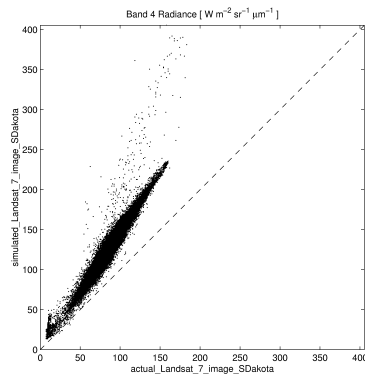


Figure 5. Radiance scatter plot showing IKONOS-derived Landsat simulation radiance values using original IKONOS radiometric coefficients vs. actual coincident Landsat ETM+ radiance values for the NIR band.

## 5. SUMMARY

The Applications Research Toolbox, developed at NASA's Stennis Space Center, provides an ability to simulate remote sensing data to assist sensor design and applications trade studies. Through simulation, data requirements can be assessed against application and research needs. Such data requirements analysis not only affects design but also has implications for sensor and data calibration and validation. Through simulation, data of varying radiometric, spatial and geometric parameters and accuracies can be produced. The various simulated products can then be assessed against a series of application needs. Such assessments, combined with cost/price considerations, can help to optimize a sensor's design, operations and calibration.

## REFERENCES

Blonski, S., 2001. IKONOS-based Simulations of Landsat 7 VNIR Data: Comparison with Actual, Coincident Images. In: *Proceedings of the 2001 High Spatial Resolution Commercial Imagery Workshop*, March 19-21, Greenbelt, Maryland.

Blonski, S., Gasser, G., Russell, J., Ryan, R., Terrie, G., Zaroni, V., 2002. Synthesis of Multispectral Bands from Hyperspectral Data: Validation Based on Images Acquired by AVIRIS, Hyperion, ALI, and ETM+. In: *Proceedings of the*

*2002 AVIRIS Earth Science and Applications Workshop*, March 5-8, Pasadena, California.

Gasser, G., 2001. *Applications Research Toolbox Technology Overview*. NASA Earth Science Applications Directorate, John C. Stennis Space Center.

## ACKNOWLEDGEMENTS

This work was supported by the NASA Earth Science Applications Directorate under contract number NAS 13-650 at the John C. Stennis Space Center, Mississippi.